Biogeosciences, 6, 275–284, 2009
www.biogeosciences.net/6/275/2009/

Biogeosciences

Towards spatial assessment of carbon sequestration in peatlands: spectroscopy based estimation of fractional cover of three plant functional types

G. Schaepman-Strub[1,2], J. Limpens[1], M. Menken[1], H. M. Bartholomeus[2], and M. E. Schaepman[2]

[1]Nature Conservation and Plant Ecology Group, Wageningen University, Wageningen, The Netherlands
[2]Centre for Geo-information, Wageningen University, Wageningen, The Netherlands

Received: 11 February 2008 – Published in Biogeosciences Discuss.: 1 April 2008
Revised: 14 January 2009 – Accepted: 21 January 2009 – Published: 25 February 2009

Abstract. Peatlands accumulated large carbon (C) stocks as peat in historical times. Currently however, many peatlands are on the verge of becoming sources with their C sequestration function becoming sensitive to environmental changes such as increases in temperature, decreasing water table and enhanced nitrogen deposition. Long term changes in vegetation composition are both, a consequence and indicator of future changes in C sequestration. Spatial continuous accurate assessment of the vegetation composition is a current challenge in keeping a close watch on peatland vegetation changes. In this study we quantified the fractional cover of three major plant functional types (PFTs; *Sphagnum* mosses, graminoids, and ericoid shrubs) in peatlands, using field spectroscopy reflectance measurements (400–2400 nm) on 25 plots differing in PFT cover. The data was validated using point intercept methodology on the same plots. Our results showed that the detection of open *Sphagnum* versus *Sphagnum* covered by vascular plants (shrubs and graminoids) is feasible with an R^2 of 0.81. On the other hand, the partitioning of the vascular plant fraction into shrubs and graminoids revealed lower correlations of R^2 of 0.54 and 0.57, respectively. This study was based on a dataset where the reflectance of all main PFTs and their pure components within the peatland was measured at local spatial scales. Spectrally measured species or plant community abundances can further be used to bridge scaling gaps up to canopy scale, ultimately allowing upscaling of the C balance of peatlands to the ecosystem level.

Correspondence to: G. Schaepman-Strub (gabriela.schaepman@wur.nl)

1 Introduction

Peatlands have been widely recognized as one of the world's largest terrestrial stores of organic C (Botch et al., 1995; Turunen et al., 2002). The extensive peat deposits show the historical role of peatlands as sinks for atmospheric C, but at the same time also show the potential of these ecosystems as sources for greenhouse gases, such as CO_2 and CH_4. As a substantial part of the peatlands can be found on the Northern Hemisphere, especially in the region where large changes in temperature, precipitation and nitrogen (N) deposition are expected, the response of peatlands to environmental change has warranted much scientific attention (Bubier et al., 2007; Limpens et al., 2008; Moore et al., 2002; Wiedermann et al., 2007).

Most studies indicate that major changes in C sequestration rate coincide with changes in vegetation composition (Strack et al., 2006). In general decreases in water table, increases in temperature as well as enhanced N deposition favour vascular plant species and, ultimately, have a negative impact on the bryophyte community through increased competition for light (Bubier et al., 2007; Wiedermann et al., 2007). Furthermore, increases in nutrient concentration and temperature seem to favour graminoid species over ericoid species (Weltzin et al., 2000, 2003). As bryophytes and vascular plants differ in their litter degradability (Dorrepaal et al., 2005), changes in their fractional covers may have direct repercussions for the ecosystems longer term C sequestration rate. Particularly the cover and productivity of the bryophyte component, dominated by the genus *Sphagnum* (Bubier et al., 2007), is of major importance to the C sequestration potential of the ecosystem. *Sphagnum* is the main peat former due to its recalcitrant litter and acts as an

Published by Copernicus Publications on behalf of the European Geosciences Union.

ecosystem engineer dictating the growth environment of vascular plants by regulating the surface hydrology and nutrient availability to a large extent (Belyea and Baird, 2006). On the whole, the biomass and the PFT fractional cover of bryophytes, graminoids and ericoid shrubs give a fair indication of the current C sequestration potential, while changes in the PFT fractional cover may serve as an early warning system for ensuing changes in C sequestration on the longer term. In addition the recognition of pure *Sphagnum* patches in a peatland vegetation may be used in the assessment of near-surface wetness (Harris et al., 2006), which exerts an important control on the C balance of peatland soils (Belyea et al., 2006; Robroek et al., 2008). Dry conditions may lead to dramatic reductions in *Sphagnum* growth rates and C fixation. Near-surface water content is an indicator of the thickness of the unsaturated zone in peat soils and thus relates to the aerobic (fast) versus anaerobic (slow) decay rates in peatland soils. Finally the near-surface wetness is related to the water table below the peatland surface, determining the size of the unsaturated zone. A thin unsaturated zone generally leads to a higher CH_4 flux from the peatland surface.

The main three PFTs in peatlands (mosses, grasslike species (graminoids), shrubs) represent groups of different structure and biochemistry, such as leaf construction (mosses lacking a vascular system, versus vascular plants), water and pigment content, and architecture. These differences result in distinct spectral characteristics at leaf and canopy level, such as the reflectance peak around 640 nm for red *Sphagnum* species and the low NIR reflectance of the ericoids (ericaceous species). Various studies highlight the spectral reflectance properties of *Sphagnum* mosses and the influence of the water content and moisture conditions on their reflectance under laboratory conditions (Bryant and Baird, 2003; Bubier et al., 1997; Harris et al., 2005; Vogelmann et al., 1993). Only few studies analysed spectrometer data of peatlands at the ecosystem scale, thus including mixtures of *Sphagnum*, shrub, graminoid, and tree cover. Harris et al. (2006) inferred proxies for near-surface wetness to map effects of water stress on *Sphagnum*, based on a variety of field and airborne sensors (Milton et al., 2008), including an Analytical Spectral Device (ASD) FieldSpec Pro spectroradiometer and the Compact Airborne Spectrographic Imager (CASI). Recently, tree and shrub leaf area indices were inferred for a peatland through an approach combining in situ leaf area index (LAI) measurements, field spectrometer data, and Landsat TM imagery (Sonnentag et al., 2007). Spectral differences between vegetation types were successfully used in other ecosystems, such as floodplains, to produce vegetation maps of structurally or chemically divergent vegetation based on imaging spectrometer data (Schaepman et al., 2007). Plant pigment and non-pigment retrieval at leaf and canopy level are becoming increasingly possible (Ustin et al., 2008), resulting in spatially distributed and continuous vegetation characteristics that can then be assimilated into process-oriented ecosystem models or regional climate models to overcome the limitations as given by maps with discrete land cover classes (Schaepman, 2007). Before employing coarser resolution imaging spectrometer over peatland areas to map the vegetation composition, it is therefore useful to compile a spectral library in situ, allowing to constrain model inversion approaches for inferring fractional abundance or biochemistry, or assess the scalability of the approach from plant to canopy level (e.g. Kalacska et al., 2007; Bojinski et al., 2003).

In this study we establish a non-destructive methodology to derive fractional cover and biomass of the main PFTs within peatlands (*Sphagnum*, graminoids, and ericoid shrubs) using field spectroscopy. To this end we selected field plots differing in PFT fractional cover and related spectral reflectance data of these plots with fractional cover estimates inferred from point intercept data and destructive measurements on dry biomass.

2 Materials and methods

2.1 Test site and set-up

Late spring 2006 we selected 25 plots (50×50 cm) differing in PFT cover at Reigersplas (52°50′N, 6°27′E), the Netherlands. The Reigersplas is located in the northeast of the Netherlands in the National Park Dwingelderveld, and is a wet heath with patches of ombrotrophic (rain-fed) peatland vegetation. Five plots (1–5) were selected within the ombrotrophic patches along five transects (A–E), situated along the water table gradient, going from relatively wet plots that were mostly dominated by *Sphagnum* with sparse graminoid cover to relatively dry plots with a continuous *Sphagnum* cover that were dominated by ericoids (Fig. 1). In between these extremes we selected plots co-dominated by ericoids and graminoids. All plots had a (near) continuous *Sphagnum* layer (>90% cover), with one exception with c. 80% *Sphagnum* cover (plot A5). Brown mosses are neglected in this study as they are not abundant in the observed ombrotrophic patches. The majority of plots were dominated by either *Sphagnum magellanicum* (Brid.) or *Sphagnum papillosum* (Lindb.), two plots being co-dominated by both species (plots C4, D2). Taken over all plots, fractional cover of vascular plant species ranged from < 5% to 99%. In order of importance ericoid species were *Erica tetralix* (L.) and *Vaccinium oxycoccus* (L.) with some *Andromeda polifolia* (L.) and *Empetrum nigrum* (L.). Graminoids comprised *Eriophorum angustifolium* (Honck.) and *Molinia caerulea* (L.).

2.2 Fractional cover determination based on point intercept method

After selection of the plots, the point intercept method (Jonasson, 1988) was used to measure the fractional cover of vascular plants and of *Sphagnum* between 22 May and 4 June 2006. This entailed fixing of a frame of 25 cm×37.5 cm

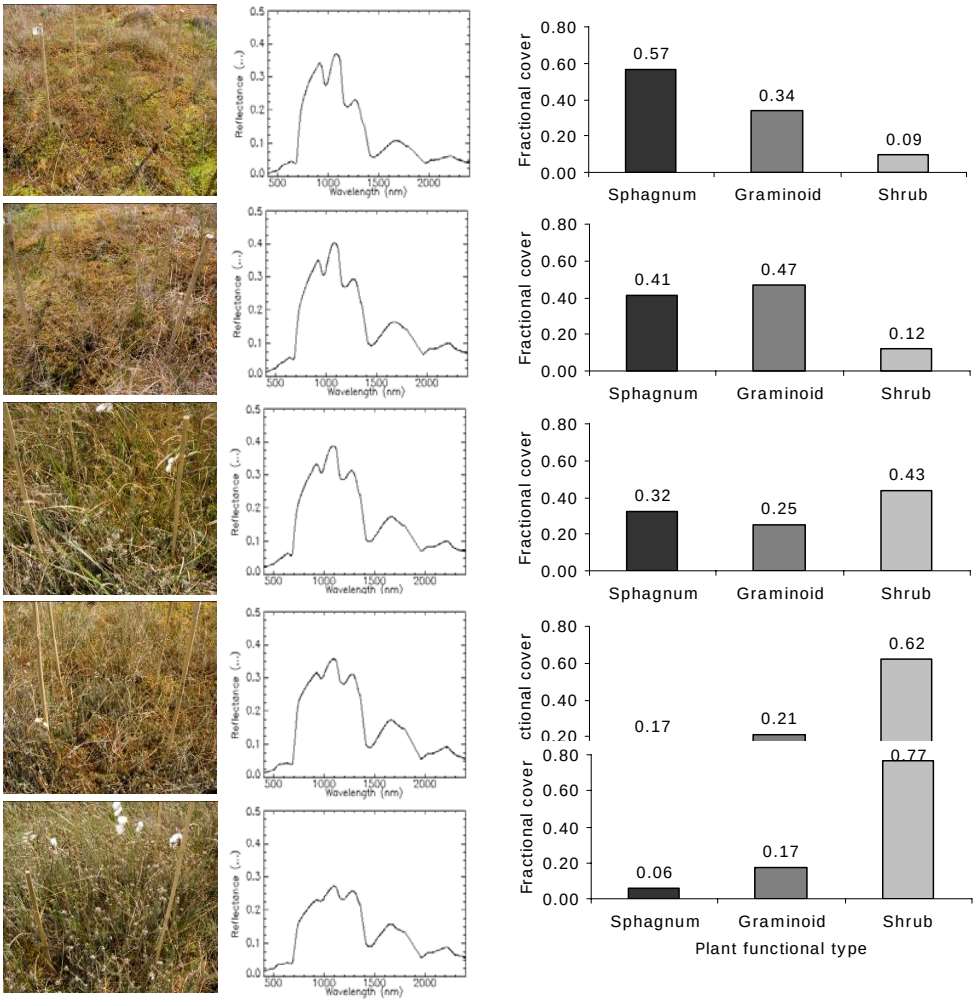

Fig. 1. Photographs of the plots of the transect E (left) with corresponding hemispherical-conical reflectance factor data (middle) and fractional cover as inferred from point intercept measurements (right) showing the changing abundance of PFTs and the effect on the reflectance spectrum at the plot level. The transect starts with a lawn with high *Sphagnum* cover close to the water table (top) and ends with a drier hummock plot with high shrub fractional cover (down).

and with a 2.5 cm grid above the vegetation. At 150 points, a stainless steel needle was lowered vertically to the vegetation canopy. We recorded the first plant species that was touched with the point of the needle ("first-hit data"), and further distinguished between living and dead material. This dataset therefore mostly relates to the fractional cover as inferred from a photograph taken above the canopy. It does not directly relate to the LAI or biomass, as the layers growing below the highest canopy layer are not taken into account. For the chosen experimental plots this means that the continuous *Sphagnum* layer, even though present in all plots (see Sect. 2.1), is only recorded if no ericoid or graminoid leaves are covering it.

2.3 Biomass sampling

On 5 June 2006, the total aboveground vegetation in each plot was cut flush with the top of the *Sphagnum*. The litter scattered on the *Sphagnum* surface was also collected. Hereafter one *Sphagnum* sample (diameter 5cm, depth 7cm) was cut from the bryophyte layer of each plot. The harvested plants (dead and living) were sorted into PFTs and dried at 70°C for 48 h before dry weight was determined.

2.4 Field spectrometer data collection and preprocessing

On 4 June 2006, the canopy reflectance (350–2500 nm) of the 25 plots was measured using an ASD Fieldspec Pro spectroradiometer (Analytical Spectral Devices, Inc. Boulder, USA). In each plot, 5 measurements were taken. The fibre optic head was mounted at 65 cm height on a tripod; care

was taken that no shade was cast on the measurement area. Using the instrument's 25° field of view (FOV), the ground field of view (GFOV) covered was approximately 29 cm in diameter. To reduce the impact of changing irradiance conditions throughout the day, a reference spectrum was collected from a white spectralon panel before the measurement of each plot. Following the terminology of Schaepman-Strub et al. (2006), the data acquired with the field spectrometer correspond to hemispherical-conical reflectance factors (HCRF). No further corrections for the changes in solar zenith angle, or partitioning of the direct to diffuse irradiance were performed.

On 08 June, 2006, spectral reflectance measurements were taken from the dominant species to obtain pure endmember spectra, following the same measurement protocol as 4 June 2006. To this end homogeneous vegetation outside the previously measured mixed plots was selected with a high fractional cover (>80%) of the target species.

The spectra were visually controlled for their quality and measurements outside one standard deviation of the five measurements per plot were excluded. The remaining measurements of each plot were averaged to the final plot spectrum. Wavelength regions influenced by atmospheric water vapour were excluded from further analysis. This resulted in a wavelength range of 400–1360 nm, 1410–1800 nm, and 1960–2400 nm (1793 spectral bands in total) used in the data analysis.

2.5 Linear spectral unmixing

Spectral mixing analysis is based on the assumption that the reflectance of an observed surface is a combination of the reflectance of the single components of the surface, weighted according to their abundance (Adams et al., 1986; Roberts et al., 1993). In most studies it is further assumed that this mixture is linear and that the multiple scattering is negligible. The model can be expressed as

$$R_{\lambda,\mathrm{obs}} = \sum_{i=1}^{N} f_i \times R_{\lambda,i} + \varepsilon_\lambda \quad (1)$$

where $R_{\lambda,\mathrm{obs}}$ is the observed reflectance factor of the surface in the spectral band λ, f_i is the fraction of the endmember, N is the number of endmembers, and ε_λ is the residual error. The inversion of the forward model, called umixing, is based on the minimization of the root mean squared error (RMSE). The quality of the unmixing is indicated by the RMSE of the model fit over all spectral bands (M), calculated as

$$\mathrm{RMSE} = \sqrt{\frac{\sum_{\lambda=1}^{M} (\varepsilon_\lambda)^2}{M}} \quad (2)$$

Based on the above assumptions, we hypothesize that the fractional cover of the single species, resulting from the linear unmixing of the reflectance of the GFOV, would equal the fractional cover as recorded by the first-hit data using the point intercept methodology.

Slightly differing implementations of the unmixing approach exist (Plaza et al. 2004). We evaluated the linear unmixing algorithm as implemented in ENVI© (ITT Vis, Boulder, USA) which did not reveal satisfactory results. An alternative unmixing algorithm is the multiple endmember spectral mixture analysis (MESMA) (Roberts et al., 1998). Within MESMA, three endmember groups may be defined, each containing a set of pure spectra. The algorithm searches for the best spectrum within each endmember group. Thus, a number of slightly varying spectra per endmember can be indicated, reflecting the natural variability of an endmember, which is not possible in simple mixture analysis. MESMA thus allows a different set of endmember spectra for each observed mixed reflectance, rather than using a common, fixed set of endmembers for all spectra in the inversion (for a detailed discussion on advantages of MESMA compared to simple linear mixture models see Roberts et al., 1998).

We used the MESMA algorithm as implemented in the Viper Tools version 1.4 (http://www.vipertools.org), which is an ENVI© software plug-in, to infer the fractional cover of the three PFTs based on the measured plot hemispherical-conical reflectance factors (HCRF's) (Schaepman-Strub et al., 2006). The minimum non-shade fraction was constrained to 0, the maximum non-shade fraction to 1. Negative fractions were allowed for the shade endmember. No further restrictions were applied (e.g. RMSE, max. shade fraction, max. residual). The MESMA output contains the model assigned according to the best fit to the plot level spectrum (i.e. the name of the endmember spectra chosen for the best fit), the abundances of each of the endmember spectra, as well as the mean error of the model fit (RMSE). The algorithm also indicates cases for which no model could be assigned with the indicated constraints.

2.5.1 Endmember selection and aggregation for fractional cover estimation

Apart from the mixed species spectra measurements along the water table gradient, we performed additional HCRF measurements on vegetation patches with single dominant species coverage to obtain pure reflectance spectra. For *Sphagnum* we selected two homogenous plots of the red species *S. magellanicum* and one of the green species *S. fallax* (Fig. 2a). The *S. magellanicum* endmember clearly showed the red reflectance peak around 636 nm, while the green peak of the *S. fallax* endmember was very broad compared to vascular plants. Further, the *Sphagnum* canopies did not show a steep red edge with a clear NIR shoulder, showed a higher reflectance peak in the near infrared, and had a lower reflectance in the covered shortwave infrared (1400–2400 nm) than green vascular plants (e.g. *Molinia* green). Strong water related features were seen at 970 nm, 1200 nm, 1450 nm. Because the measurements were performed in late

Table 1. Endmember provided for the MESMA procedure. From each endmember group (i.e. mosses, graminoids, and shrubs), one endmember is selected by MESMA leading to the best plot level spectrum fit. The forth endmember is a photometric shade (zero reflectance in all spectral bands).

Endmember groups	Endmembers	Species
1st EM *Sphagnum*	sm1	*Sphagnum magellanicum*
	sm2	*Sphagnum magellanicum*
	sf	*Sphagnum fallax*
2nd EM graminoids	ea1	*Eriophorum angustifolium*
	ea2	*Eriophorum angustifolium*
	mc_green	*Molinia caerulea green*
	mc_brown	*Molinia caerulea brown*
3rd EM shrubs	et1	*Erica tetralix*
	et2	*Erica tetralix*
	vo	*Vaccinium oxycoccus*
4th EM shade	shade	Photometric shade

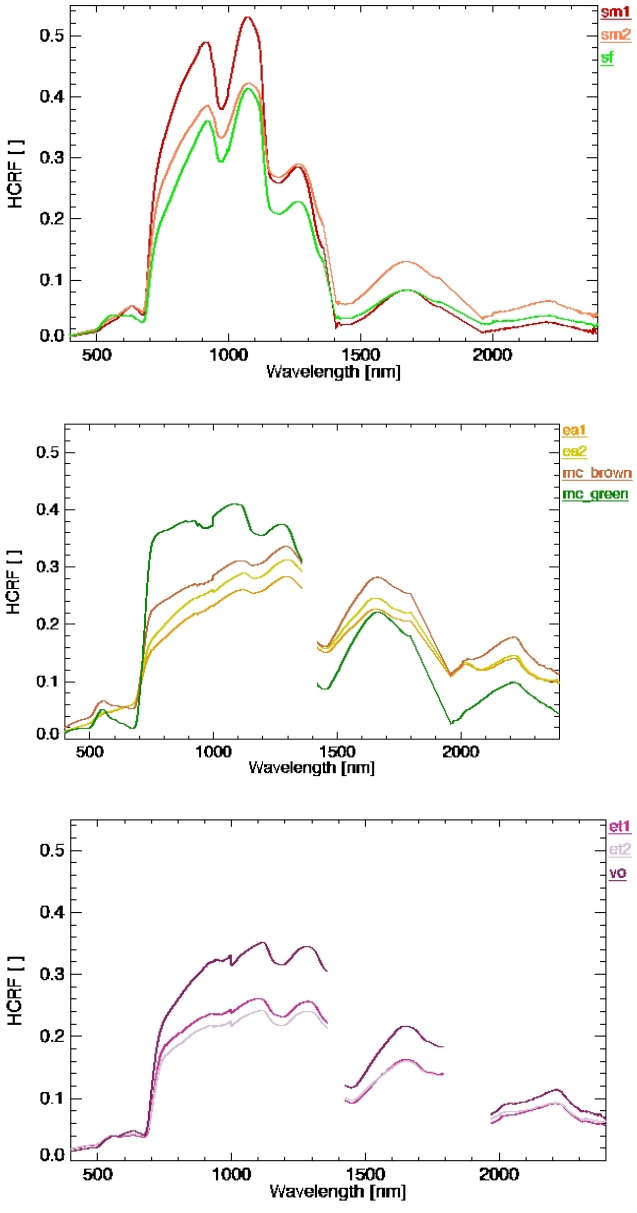

Fig. 2. Endmember spectra for the MESMA algorithm. The *Sphagnum* endmember (top) was selected from *Sphagnum magellanicum* (sm) and *fallax* (sf); the graminoid endmember (middle) from *Eriophorum angustifolium* (ea), *Molinia caerulea* with green biomass (mc_green) and dead biomass (mc_dead); and the shrub endmember (bottom) from *Erica tetralix* (et) and *Vaccinium oxycoccus* (vo). Additionally, a photographic shade endmember was used with a zero reflectance value for all wavelengths (not shown).

spring, the dead fraction in graminoid-dominated plots was still very high. We therefore selected one spectrum for pure *Molinia* green biomass and one for *Molinia* litter. Additionally we had two spectra for *Eriophorum*, containing standing dead and living biomass (Fig. 2b). Except for the green *Molinia*, all graminoid endmembers contain dead biomass expressed by the relatively weak absorption around 680 nm which is usually more pronounced by chlorophyll a absorption, the low near-infrared reflectance, and the almost missing water absorption features. For the ericoid shrubs we obtained a spectra covering a mixture of ericoids, but dominated by *Vaccinium oxycoccus*, and two pure spectra from relatively high *Erica* vegetation (Fig. 2c). The pure ericoid endmember spectra show a very low reflectance in the near infrared compared to *Sphagnum* and graminoids.

The single species reflectance spectra were grouped by their PFT, resulting in three vegetation endmembers and one endmember representing photometric shade (an option in the MESMA algorithm with a zero reflectance throughout all wavelengths). The MESMA algorithm selects the spectrum of the dominant species within each PFT for the unmixing procedure (Table 1). The set of provided endmembers (3 for *Sphagnum*, 4 for graminoids, 3 for shrubs, one for shade) leads to a total of 36 potential endmember models ($3\times4\times3=36$) which can be assigned to a plot level spectrum. We thus assumed that in each plot one species is representing the fractional cover of the entire PFT. This may lead to higher RMSE values of the model fit when the reflectance of the species within one PFT varies significantly.

Brightness variations of the spectra of a given vegetation canopy under stable atmospheric conditions can be related to the anisotropic reflectance properties of the canopy, whereas three main factors are important, namely the sun angle, the viewing geometry, and the structure of the canopy (i.e. the density and distribution (vertical and horizontal) of the scattering components). Since our measurements are taken with constant viewing angle and under limited changes in solar angle, variations of the fraction of shade for different sites are mainly related to differences in canopy structure. Further,

Table 2. Results of the three MESMA scenarios (1 – all plots with assigned model, 2 – results with RMSE >0.001 excluded, 3 – wavelength restriction to 400–1000 nm) and corresponding correlation with fractional cover as inferred from the point intercept methodology (PI) for the three PFTs (the MESMA inferred shrub fraction includes the shade fraction for all 3 scenarios). In the PI-MESMA correlation equation, x refers to point intercept data and y to MESMA inferred fractional cover data.

	Scenario 1	Scenario 2	Scenario 3
MESMA			
No. plots	23	21	24
Mean RMSE	0.0056	0.0050	0.0045
PI–MESMA			
Sphagnum	R^2=0.76	R^2=0.81	R^2=0.47
	y=0.8548x+0.0418	y=0.9576x+0.0194	y=0.6913x+0.0218
Graminoids	R^2=0.54	R^2=0.57	R^2=0.11
	y=0.975x+0.0177	y=0.9882x+0.0275	y=0.628x+0.2396
Shrubs	R^2=0.43	R^2=0.54	R^2=0.39
	y=0.5784x+0.1549	y=0.701x+0.0881	y=0.7168x+0.0548

the shaded background is constant, given the high *Sphagnum* cover below the ericoids. Ericoid shrubs with their branches and thick leaves are assumed to be the main shadow-casting components for our site (as compared to *Sphagnum* and graminoids).The shrubs cast most of the shadow due to their height and loose canopy, further the ericoids showed the lowest HCRF values, thus being closest to the zero reflectance spectrum of the shade. We therefore added the shade abundance results to the shrub abundances for the comparison with the point intercept methodology data.

Three main scenarios are discussed in the results, namely:

Scenario 1 including all plot results where an endmember model was assigned.

Scenario 2 excluding plot results with a high RMSE. The corresponding threshold is set as the mean RMSE of all plots plus 2 times the standard deviation.

Scenario 3 results are inferred from a MESMA run restricted to the wavelength 400–1000 nm. This reveals whether the visible spectral range contains enough information compared to the full wavelength range (400–2400 nm) of Scenario 1.

The linear spectral mixing model is a physically based model and resulting abundances directly relate to the components occurring within the field of view. The results therefore do not need a calibration to retrieve physical quantities. To validate obtained fractions, we compared the endmember abundances resulting from MESMA to fractional cover as inferred from first-hit point-quadrat data. The validation reveals limitations and uncertainties of the approach and assumptions made.

2.5.2 Relation of fractional cover and biomass

The fractional cover results are used in a final step to investigate their relation with dry biomass data. We therefore analyze the relation of both, point-quadrat first hit data and fractional cover inferred from MESMA, with destructively measured biomass.

3 Results

3.1 MESMA results

3.1.1 Scenario 1 results (plots with assigned endmember model)

Out of 36 potential endmember models, 13 were identified by the MESMA algorithm to fit the 25 observed plot HCRF data. No specific pattern in the model selection could be found, apart from the fact that the green *Molinia caerulea* and the *Vaccinium oxycoccus* were only included in 4 and 3 cases, respectively. For two plot spectra, no appropriate model could be assigned within the given constraints (transect A, plot 1 and 4), leading to a final number of 23 plots with successfully assigned abundances. The reason for A1 (*Sphagnum* cover of 0.68 by point intercept method) was that the observed plot level spectrum had higher values than the available *Sphagnum fallax* endmember, while the *S. magellanicum* endmember showed a higher reflectance but did not fit the shape in the green and red spectral bands due to the red reflectance peak. Generally, the obtained fits were very good, with a low RMSE ranging from 0.0027 to 0.0118, exceeding 0.01 in two cases only. The mean RMSE over all assigned plots (23) was 0.0056.

3.1.2 Scenario 2 results (plots with assigned endmember model and high RMSE)

Based on the mean (0.0056) and standard deviation (0.0027) of the RMSE of all plots, the RMSE threshold (mean RMSE

of all plots plus 2 times the standard deviation) was set to 0.011, leading to the exclusion of two plots. The mean RMSE over the remaining 21 plots was 0.0050.

3.1.3 Scenario 3 results (MESMA run based on visible spectral range)

Scenario 3 revealed how important the infrared spectral range is for inferring the fractions of the three PFTs within the test site. Only for a single plot spectrum no corresponding endmember model was assigned, whereas the RMSE was higher than 0.01 for three plots. The mean RMSE over all assigned plots (24) was 0.0045, thus slightly lower than for Scenario 1 and 2.

3.2 Fractional cover

3.2.1 Scenario 1 results (plots with assigned endmember model)

For *Sphagnum*, the fractional cover estimate using field spectroscopy was in agreement with the point intercept method (R^2=0.76) and close to the 1:1 line, yielding a high *Sphagnum* cover under open vascular plant canopy and a low *Sphagnum* cover under dense vascular plant canopy. The absolute *Sphagnum* cover in all plots was generally >90% (see Sect. 2.1). The above result shows that the fractional cover as inferred from the MESMA procedure corresponds to the first-hit data, this means that the *Sphagnum* abundance below a dense graminoid or ericoid canopy cannot be inferred. On the other hand, in case of loose vascular plant canopies, a dense *Sphagnum* background may lead to an underestimation of the graminoid and ericoid fractional cover compared to first hit data, as adjacency effects may lead to an overrepresentation of *Sphagnum* in the mixed signal.

For graminoids, the agreement between both methods was less strong (R^2=0.54) (Table 2), with the field spectroscopy method giving a higher estimate at low covers and a lower estimate at dense cover. Graminoids were not well developed in June yet, and contained a high fraction of dead standing litter for some species which might not be well represented in the graminoid endmember spectra.

For the ericoid shrubs, the agreement between the two methods was weak (R^2=0.19) when the shade fraction was not assigned to the shrub fraction. When summing up the shrub and the shade fraction, the agreement between point intercept and field spectroscopy inferred results was much higher (R^2=0.43).

The field spectroscopy method generally yielded a higher estimate at low cover and a lower estimate at dense cover, although the deviation from the 1:1 line was less than for the graminoids.

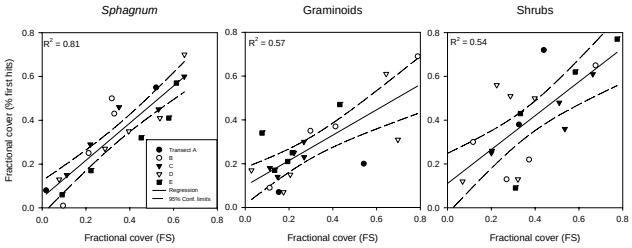

Fig. 3. Relationship between fractional cover estimates using point intercept method (Fractional cover (% first hits) and field spectroscopy (Fractional cover – FS) for 3 PFTs following Scenario 2.

3.2.2 Scenario 2 results (plots with assigned endmember model and high RMSE)

The exclusion of plot results showing a model fit significantly deviating from the mean (i.e. RMSE>0.011) lead to an improved fit with the point intercept methodology (Table 2). The correlations improved to R^2=0.81 for *Sphagnum*, R^2=0.57 for graminoids, and R^2=0.54 for shrubs with significance levels of p=0.002, p<0.001, and p<0.001, respectively (Fig. 3). Further, the fit equations move closer to a 1:1 relationship for all three PFTs (Table 2). When summing up the shrub and graminoid fractions to a vascular plant fraction, the point intercept and MESMA inferred results correlate with a similar fit (R^2=0.82). The small difference between the *Sphagnum* and the vascular plant fit quality can be explained by the RMSE.

It should be noted that the exclusion of the two data points relies on a statistical quality measure of the fit of the MESMA procedure and is not based on any information inferred from the point intercept methodology. The RMSE can be used as a quality measure to identify outliers – if the spectrum cannot be reasonably explained by provided endmembers, the RMSE will deviate from the mean RMSE and corresponding results need further investigation.

3.2.3 Scenario 3 results (MESMA run based on visible spectral range)

Even though the MESMA quality indicators are good, the poor correlation results of the fractional cover with data from the point intercept methodology (e.g. R^2=0.47 for *Sphagnum*, Table 2) show how important the longer wavelength ranges (i.e. near-infrared and shortwave infrared) are to distinguish between PFTs in peatlands. *Sphagnum* shows distinct water absorption features in the longer wavelength range due to its high water holding capacity, and pigmentation alone in the visible range is not sufficient to distinguish between the three PFTs.

3.3 Biomass

The MESMA fractional cover based on Scenario 2, as well as the fractional cover inferred from point intercept data were finally correlated to the biomass.

For *Sphagnum* there was no relationship ($R^2 \leq 0.03$) between fractional cover and biomass, irrespective of the method used (Fig. 4 top). This result is expected as the *Sphagnum* shielded by the graminoid and ericoid leaves was not detected by both methods, while it contributes considerably to the biomass.

For graminoids however, biomass was surprisingly well related (R^2=0.57) to the fractional cover estimate derived from field spectroscopy, but not to the estimate derived from the point intercept method (R^2=0.26). The graminoid fractional cover as inferred by MESMA varies between 0.02 and 0.7, with an average value of 0.28. This intermediate vegetation density allows getting a rough approximation of the biomass through the fractional cover as inferred from MESMA.

For the ericoid shrubs, there was an opposite response. Here biomass was better predicted by the fractional cover estimate derived from the point intercept method (R^2=0.44), than by the estimate derived from field spectroscopy (R^2=0.14).

When again summing up the shrub and graminoid fraction for the point intercept and MESMA approach, they showed an improved correlation with the biomass of R^2=0.65 and R^2=0.60, respectively.

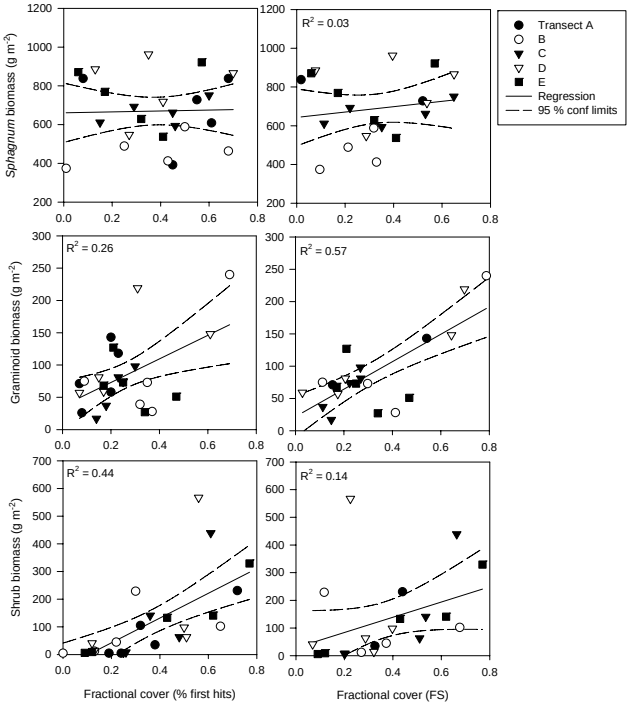

Fig. 4. Relationship for three PFTs between fractional cover estimates and biomass for point intercept method (left) and field spectroscopy (right). Biomass refers to aboveground dry biomass for graminoids and shrubs and upper 7 cm for *Sphagnum*.

4 Discussion and conclusions

The application of the MESMA algorithm has proven to be an appropriate methodology to separate *Sphagnum* from vascular plant fractional cover in the selected peatland test site. The low RMSE values obtained show that generally the selected endmembers and corresponding abundances fit well with the plot level spectrum. This result is certainly influenced by the fact that all spectra were obtained with the same instrument and thus same spatial and spectral resolution and under comparable solar angles and weather conditions. Unlike earlier studies, we present reflectance spectra of all PFTs of peatlands under natural illumination conditions as mixture and in pure species coverage.

Compared to the endmembers used by Sonnentag et al. (2007), the *Sphagnum* versus vascular plant endmembers of this study show different reflectance behaviour. In our dataset, the *Sphagnum* reflectance is generally higher than most vascular plant spectra in the spectral range of the Landsat TM band 4 (760–900 nm), and always lower in band 5 (1550–1750 nm) and 7 (2080–2350 nm), while it is the opposite in the Sonnentag et al. (2007) study. This opposite reflectance behaviour may partly stem from the different species and structure of the canopy, because the study site of Sonnentag et al. (2007) included also tree species which were not present in our case. On the other hand it should be noted that they inferred the moss endmembers from field spectrometer data while the vascular plant endmember is based on the TM image. Different scattering and adjacency effects present in field and satellite measurements, even when compensated properly for atmospheric effects and illumination geometries, may result in biases which do not relate to inherent properties of the PFTs. As the endmembers are crucial for the MESMA procedure, it is recommended to carefully investigate their consistency and reliability for the corresponding test site.

The wavelength test shows that with visible and NIR wavelengths only, the MESMA algorithm finds mathematically suitable solutions to the inversion problem, expressed by the relatively low RMSE. However, the resulting abundances do not correlate well with the fractional cover as inferred from the point intercept methodology. This is an important finding for upscaling purposes, as many of the operational and higher resolution satellites (e.g. Landsat ETM+ and TM) do not cover the spectral range of the well-defined water absorption bands shown by the *Sphagnum* endmember. Nevertheless a combination of the green, NIR and SWIR band might still lead to satisfactory results. However, this means that the absolute reflectance values of the endmembers

have to be determined very carefully as the water absorption feature cannot contribute to identify the properly matching endmembers. This shows the need to perform more detailed analysis when reducing the spectral resolution for the MESMA procedure.

This study demonstrated that based on spectrometer data, *Sphagnum* fractional cover can successfully be distinguished from vascular plant fractional cover. However, the partitioning of the vascular plant fractional cover into a shrub and graminoid fraction was less successful and needs further work with respect to endmember measurements. This includes the measurement of shade endmembers to replace the photometric shade which is wavelength independent, as well as a careful experimental setup in terms of solar angle and corresponding reflectance anisotropy effects.

We acknowledge that under less optimal conditions (e.g., very noisy data, less optimal endmember selection (such as not covering all abundant *Sphagnum* communities), or using airborne data without atmospheric compensation), higher uncertainties might result due to further increasing the ill-posedness of the inverse problem. It is only recommended to transfer the presented endmember spectra or correlations as presented in Table 2 to other research sites, when working with similar abundances of species. Otherwise we suggest adapting the analysis to the area of interest by using in situ endmember reflectance spectra; or alternatively, laboratory measured endmember spectra of individual species.

The above results lead to the following conclusions for the application to assess and predict the C cycle in peatlands:

1. The presented methodology can be used to map open *Sphagnum* patches and consequently apply a water-based index on the pure *Sphagnum* spectra as a proxy for the near-surface hydrological conditions to detect drought conditions (methodology as presented in Harris et al. (2006)). Reduction of the near-surface water content can lead to a reduction in rates of *Sphagnum* growth and therefore, C fixation. Harris et al. (2006) mentioned that their *Sphagnum* mapping procedure, based on a mixed tuned match filtering approach, was largely an iterative process and may increase user bias and reduce accurate repeatability due to the manual adjustment of the threshold. After the careful selection of the endmembers, the MESMA approach applied in this study proved to be very stable, and revealed reasonable results even without application of a threshold. Applying a standard threshold to the product quality output (mean RMSE plus 2 standard deviations) resulted in an R^2=0.81 for *Sphagnum* and R^2=0.82 for vascular plants (sum of shrub plus ericoid fractional cover) when compared to point intercept methodology data.

2. The partitioning of the vascular plant cover into shrub and graminoid fraction is still limited. This is not such a problem for boreal peatlands, where litter decomposition rates are less defined along graminoid-shrub lines. However this limitation will increase uncertainties when inferring C turnover for more temperate peatlands, as they show bigger differences in decomposition rates between graminoid and shrub litter (Dorrepaal, 2007). We see the potential to improve the pure endmembers of the shrubs as the mixed shrub endmember we used showed the influence of the *Sphagnum* reflectance. Further, the shade of the graminoids and the ericoids on different backgrounds (i.e., *Sphagnum*, graminoids, and ericoids) should be measured separately, replacing the photometric shade by a wavelength dependent shade. PFT specific shade would also partially compensate for the non-linear scattering contributions of the vegetation canopy which is currently neglected by the MESMA approach. Once the partitioning into shrubs and graminoids has improved, the fractions of the three PFTs can directly be used to assess the C sequestration potential of the observed peatland. The observation of the vegetation composition in combination with wetness indicators will lead to a better estimation of the net ecosystem CO_2 exchange as suggested by Strack et al. (2006), who emphasize the importance to combine ecological and hydrological indicators.

This study is a step towards using spatially continuous mapping of the *Sphagnum* versus vascular plant fractional cover over time to monitor potential vegetation succession as induced by changes in hydrology or nutrient availability (e.g. nitrogen deposition) and related changes in the C cycle.

Acknowledgements. The work of G. Schaepman-Strub was supported by an external fellowship of the European Space Agency.

Edited by: A. Arneth

References

Adams, J. B., Smith, M. O., and Johnson, P. E.: Spectral mixture modeling - a new analysis of rock and soil types at the viking lander-1 site, J. Geophys. Res.-Solid, 91, 8098–8112, 1986.

Belyea, L. R. and Baird, A. J.: Beyond "The limits to peat bog growth": Cross-scale feedback in peatland development, Ecol. Monogr., 76, 299–322, 2006.

Bojinski, S., Schaepman, M. E., Schläpfer, D., and Itten, K. I.: SPECCHIO: A spectrum database for remote sensing applications, Comput. Geosci., 29, 27–38, 2003.

Botch, M. S., Kobak, K. I., Vinson, T. S., and Kolchugina, T. P.: Carbon pools and accumulation in peatlands of the former soviet-union, Global Biogeoch. Cy., 9, 37–46, 1995.

Bryant, R. G. and Baird, A. J.: The spectral behaviour of *Sphagnum* canopies under varying hydrological conditions, Geophys. Res. Lett., 30(3), 1134, doi:10.1029/2002GL016053, 2003.

Bubier, J. L., Rock, B. N., and Crill, P. M.: Spectral reflectance measurements of boreal wetland and forest mosses, J. Geophys. Res.-Atmos., 102, 29483–29494, 1997.

Bubier, J. L., Moore, T. R., and Bledzki, L. A.: Effects of nutrient addition on vegetation and carbon cycling in an ombrotrophic bog, Global Change Biol., 13, 1168–1186, 2007.

Dorrepaal, E., Cornelissen, J. H. C., and Aerts, R.: Changing leaf litter feedbacks on plant production across contrasting sub-arctic peatland species and growth forms, Oecologia, 151, 251–261, 2007.

Dorrepaal, E., Cornelissen, J. H. C., Aerts, R., Wallen, B., and Van Logtestijn, R. S. P.: Are growth forms climate-independant predictors of leaf litter quality and decomposability across peatlands?, J. Ecol., 4, 817–828, 2005.

Harris, A., Bryant, R. G., and Baird, A. J.: Detecting near-surface moisture stress in *Sphagnum* spp., Remote Sens. Environ., 97, 371–381, 2005.

Harris, A., Bryant, R. G., and Baird, A. J.: Mapping the effects of water stress on *Sphagnum*: Preliminary observations using airborne remote sensing, Remote Sens. Environ., 100, 363–378, 2006.

Jonasson, S.: Evaluation of the point intercept method for the estimation of plant biomass, Oikos, 52, 101–106, 1988.

Kalacska, M., Bohlman, S., Sanchez-Azofeifa, G. A., Castro-Esau, K., and Caelli, T.: Hyperspectral discrimination of tropical dry forest lianas and trees: Comparative data reduction approaches at the leaf and canopy levels, Remote Sens. Environ., 109(4), 406–415, 2007.

Limpens, J., Berendse, F., Blodau, C., Canadell, J. G., Freeman, C., Holden, J., Roulet, N., Rydin, H., and Schaepman-Strub, G.: Peatlands and the carbon cycle: From local processes to global implications – a synthesis, Biogeosciences, 5, 1475–1491, 2008, http://www.biogeosciences.net/5/1475/2008/.

Milton, E. J., Schaepman, M. E., Anderson, K., Kneubühler, M., and Fox, N.: Progress in field spectroscopy, Remote Sens Environ, doi:10.1016/j.rse.2007.08.001, accepted for publication, 2008.

Moore, P. D.: The future of cool temperate bogs, Environ. Conserv., 29, 3–20, 2002.

Plaza, A., Martinez, P., Perez, R., and Plaza, J.: A quantitative and comparative analysis of endmember extraction algorithms from hyperspectral data, IEEE T. Geosci. Remote, 42(3), 650–663, 2004.

Roberts, D. A., Smith, M. O., and Adams, J. B.: Green vegetation, nonphotosynthetic vegetation, and soils in AVIRIS data, Remote Sens Environ, 44(2–3), 255–269, 1993.

Roberts, D. A., Gardner, M., Church, R., Ustin, S., Scheer, G., and Green, R. O.: Mapping chaparral in the Santa Monica mountains using multiple endmember spectral mixture models, Remote Sens. Environ., 65, 267–279, 1998.

Robroek, B. J. M., Schouten, M. G. C., Limpens, J., Berendse, F., and Poorter, H.: Interactive effects of water table and precipitation on net CO_2 assimilation of three co-occurring *Sphagnum* mosses differing in distribution above the water table, Global Change Biol., 14, 1–12, 2008.

Schaepman, M. E.: Spectrodirectional remote sensing: from pixels to processes, Int. J. Appl. Earth Obs., 9, 204–223, 2007.

Schaepman, M. E., Wamelink, G. W. W., van Dobben, H. F., Gloor, M., Schaepman-Strub, G., Kooistra, L., Clevers, J. G. P. W., Schmidt, A., and Berendse, F.: River floodplain vegetation scenario development using imaging spectroscopy derived products as input variables in a dynamic vegetation model, Photogramm Eng. Rem. S., 73, 1179–1188, 2007.

Schaepman-Strub, G., Schaepman, M. E., Painter, T. H., Dangel, S., and Martonchik, J. V.: Reflectance quantities in optical remote sensing–definitions and case studies, Remote Sens. Environ., 103, 27–42, 2006.

Sonnentag, O., Chen, J. M., Roberts, D. A., Talbot, J., Halligan, K. Q., and Govind, A.: Mapping tree and shrub leaf area indices in an ombrotrophic peatland through multiple endmember spectral unmixing, Remote Sens Environ, 109, 342-360, 2007.

Strack, M., Waddington, J. M., Rochefort, L., and Tuittila, E. S.: Response of vegetation and net ecosystem carbon dioxide exchange at different peatland microforms following water table drawdown, J. Geophys. Res.-Biogeosci., 111, 2006.

Turunen, J., Tomppo, E., Tolonen, K., and Reinikainen, A.: Estimating carbon accumulation rates of undrained mires in Finland - application to boreal and subarctic regions, Holocene, 12, 69–80, 2002.

Ustin, S., Asner, G., Gamon, J., Huemmerich, K., Jacquemoud, S., Zarco-Tejada, P., and Schaepman, M. E.: Retrieval of quantitative and qualitative information about plant pigment systems from high resolution spectroscopy, Remote Sens. Environ., accepted, 2009.

Vogelmann, J. E. and Moss, D. M.: Spectral reflectance measurements in the genus sphagnum, Remote Sens. Environ., 45, 273–279, 1993.

Weltzin, J. F., Pastor, J., Harth, C., Bridgham, S. D., Updegraff, K., and Chapin, C. T.: Response of bog and fen plant communities to warming and water-table manipulations, Ecology, 81, 3464–3478, 2000.

Weltzin, J. F., Bridgham, S. D., Pastor, J., Chen, J. Q., and Harth, C.: Potential effects of warming and drying on peatland plant community composition, Glob. Change Biol., 9, 141–151, 2003.

Wiedermann, M. M., Nordin, A., Gunnarsson, U., Nilsson, M. B., and Ericson, L.: Global change shifts vegetation and plant-parasite interactions in a boreal mire, Ecology, 88, 454–464, 2007.